Element-Selective Nanosecond Magnetization Dynamics in Magnetic Heterostructures

M. Bonfim,[1] G. Ghiringhelli,[2,*] F. Montaigne,[3] S. Pizzini,[1,†] N. B. Brookes,[2] F. Petroff,[3] J. Vogel,[1] J. Camarero,[1] and A. Fontaine[1]

[1]*Laboratoire Louis Néel, CNRS, 25 avenue des Martyrs, B.P. 166, 38042 Grenoble Cedex 9, France*
[2]*European Synchrotron Radiation Facility (ESRF), B.P. 220, 38043 Grenoble, France*
[3]*UMR CNRS-Thomson CSF, Domaine de Corbeville, Orsay, France*

(Received 12 October 2000)

We have developed a new original technique to study the magnetization reversal dynamics of thin films with element selectivity in the nanosecond time scale. X-ray magnetic circular dichroism measurements in pump-probe mode are carried out taking advantage of the time structure of synchrotron radiation. The dynamics of the magnetization reversal of each of the layers of complex heterostructures (like spin valves or tunnel junctions) can be probed independently. The interlayer coupling in the studied systems has been shown to play a key role in the determination of the magnetization reversal of each individual layer.

DOI: 10.1103/PhysRevLett.86.3646 PACS numbers: 78.20.Ls, 75.70.Ak, 85.70.Kh

The dynamics of the magnetization reversal in thin magnetic films has become a matter of high interest for the future of magnetic recording and nonvolatile magnetic memories. Parallel to the evolution towards smaller magnetic bits and memory cells, writing and reading times approaching the ns range will be required a few years from now [1]. While recent research in this field has concentrated on single magnetic films or microstructures [2–6], devices like spin valves and magnetic tunnel junctions [7,8] are complex heterostructures including several ferromagnetic (FM) layers. A complete understanding of the magnetization dynamics in these structures requires the ability to probe the magnetization of the individual layers as well as their mutual interaction. Magnetic coupling, either related to exchange and dipolar interactions or induced by surface roughness, is known to strongly influence the static magnetization reversal of spin valves and tunnel junctions. The influence of magnetic coupling on magnetization dynamics is not known since the experimental techniques used up to now measure either the total magnetization or the average angle between the magnetization of two FM layers. The behavior of each individual layer is thus difficult to address with these techniques.

In this Letter we demonstrate that time-resolved x-ray magnetic circular dichroism (XMCD) provides a unique experimental tool to investigate the magnetization dynamics of magnetic heterostructures with chemical selectivity. As an example, we show the results obtained on selected $Co/X/Ni_{80}Fe_{20}$ trilayers (with X = Cu or Al_2O_3), either in the form of continuous thin films or patterned in micron-sized squares. Co and $Ni_{80}Fe_{20}$ (permalloy) are typically used as hard and soft magnetic layers in spin valves (with a Cu spacer) and magnetic tunnel junctions (Al_2O_3 spacer). Spin-valve systems are based on the giant magnetoresistance effect and have already found an important application in magnetoresistive read heads [9], while magnetic tunnel junctions are intensively studied for their potential use [8] as nonvolatile magnetic memories (MRAM).

The importance of XMCD for the investigation of magnetic properties of thin layers and micro/nanostructures is well established [10]. Our time-resolved XMCD experiments were carried out on the soft x-ray beam line ID12B of the European Synchrotron Radiation Facility (ESRF). Time resolution is achieved using a pump-probe scheme [11–13], where the magnetic pulses created by a microcoil (the pump) are synchronized with the x-ray photon pulses (the probe) at the repetition frequency of the ESRF, which is 357 kHz in single bunch mode. The sample is positioned at grazing incidence in the 1 mm wide aperture of a copper microcoil [14] mounted in high vacuum. At 357 kHz, the current drivers based on fast power MOSFET transistors can give a pulsed field up to 0.1 T in the plane of the sample, with a maximum slope of 8 mT/ns. An electromagnet mounted outside the vacuum chamber provides a static bias field during the dynamic measurements and allows hysteresis cycles to be measured. The x-ray absorption is measured using a large area photodiode to detect the fluorescence yield. In contrast to electron detection, fluorescence detection allows deeply buried magnetic layers to be studied and measurements to be done in the presence of a (strong) magnetic field.

Chemical selectivity is obtained by tuning the x-ray photon energy to an absorption edge of the layer of interest. In our case, maximum sensitivity was reached using the L_3 white line of Co (778 eV) for the cobalt layer and the L_3 white line of Ni (853 eV) for the permalloy layer. The x-ray absorption of the two FM layers is measured at the selected energy as a function of the delay between the magnetic pulse and the photon bunch. The delay scan is carried out for two opposite helicities of the x-ray beam. The difference between the two scans gives the time dependence of the L_3-XMCD intensity, and therefore of the magnetization of the probed layer, during and after the application of the magnetic field pulse. The time resolution is limited by the x-ray bunch width, which is 100 ps at the ESRF.

 0031-9007/01/86(16)/3646(4)$15.00

For all the measurements reported here, the sample is first magnetically saturated in the negative direction by a static field applied along the easy magnetization axis of the sample. A negative bias field (H_{bias}) is constantly applied during the time-dependent measurements to guarantee that the system returns to negative saturation after the application of each positive field pulse (H_{pulse}).

The $Co/Cu/Ni_{80}Fe_{20}$ and $Co/Al_2O_3/Ni_{80}Fe_{20}$ trilayers we have investigated were grown on stepped Si(111) substrates [15]. They display an in-plane uniaxial magnetic anisotropy with the easy axis parallel to the steps. Patterned structures consisting of square dots of 1.3 μm side with a period of 4 μm were fabricated by Ar ion etching of the continuous $Co/Al_2O_3/Ni_{80}Fe_{20}$ films. The samples display a variety of magnetic coupling behaviors which give rise to different magnetization dynamics.

We first concentrate on magnetic tunnel junctions (MTJ) of composition $Co(15\text{ nm})/Al_2O_3(2\text{ nm})/Ni_{80}Fe_{20}(5\text{ nm})$. The two magnetic layers display a weak ferromagnetic orange-peel-type coupling with a coupling energy of about 4 $\mu J/m^2$. The preparation and the properties of these junctions are described in detail in Ref. [16]. The quasistatic coercive fields of the permalloy and Co layers are, respectively, 1.6 and 3 mT.

Figure 1 shows the time evolution of both Co and $Ni_{80}Fe_{20}$ magnetization for 30-ns-long field pulses of different amplitudes. A 5 mT static bias field was applied in the direction opposite to the pulsed field. Considering

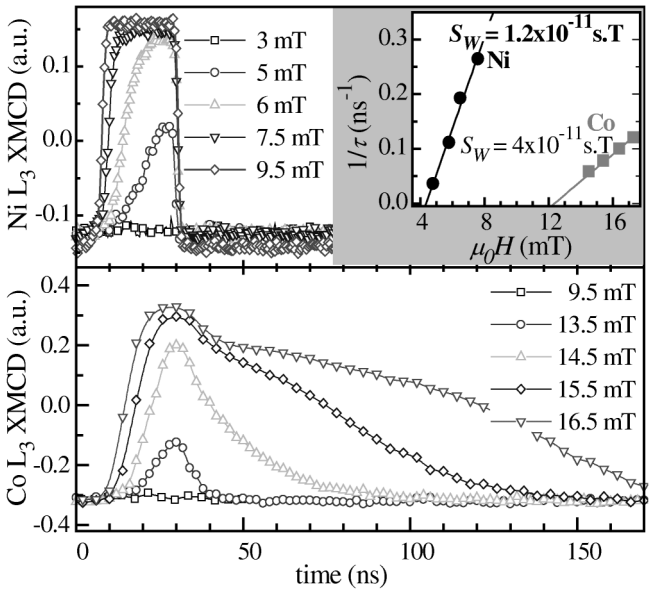

FIG. 1. Time evolution of the magnetization of the $Ni_{80}Fe_{20}$ layer (top) and the Co layer (bottom) of a $Co/Al_2O_3/Ni_{80}Fe_{20}$ tunnel junction, during and after application of 30-ns-long magnetic pulses of different amplitudes. A continuous bias field of -5 mT was applied during the measurements. The field amplitudes in the legends are ($H_{\text{pulse}} + H_{\text{bias}}$). Inset: Plot of the inverse of the reversal time ($1/\tau$) versus the field amplitude on the rising edge of the field pulse.

the 10 ns rise time of the field pulse, the initial "dead time" corresponds to the time required to overcome the reverse bias field plus the coercive field of the $Ni_{80}Fe_{20}$ layer. After this regime, the evolution on the rising edge is almost linear with time, the slope increasing with the pulse amplitude. The $Ni_{80}Fe_{20}$ magnetization completely reverses for a field of 9.5 mT, while 16 mT are needed to reverse the Co layer. The effective coercivities for these short pulses are several times larger than the quasistatic coercivities.

Let us define the switching time τ as the time needed to cancel the magnetization of the Co or of the permalloy layers. A plot of the inverse of τ versus the amplitude of the pulsed field (inset of Fig. 1) shows that the relationship

$$\tau^{-1} = S_w^{-1}(H - H_0) \tag{1}$$

is verified for both magnetic layers, with different S_w values. Here H is the applied field, H_0 is a constant field related to the coercivity, and S_w is a coefficient related to magnetic viscosity.

This empirical relationship has been shown to hold, with different switching coefficients S_w, for several mechanisms of magnetization reversal ranging from domain wall propagation (lower τ^{-1}) to uniform rotation (higher τ^{-1}) [1,17]. The values of S_w deduced from our measurements (1.2×10^{-11} s T for $Ni_{80}Fe_{20}$ and 4.0×10^{-11} s T for Co layers), compared with those reported in the literature, point to magnetization reversal dominated by nucleation of reversed domains. The possibility of reversal by coherent rotation is ruled out by the fact that the magnetic response is strongly delayed with respect to the pulsed field. The extrapolation of the fits to $\tau^{-1} = 0$ gives field values larger than the quasistatic coercive fields of the Co and $Ni_{80}Fe_{20}$ layers. This result is not surprising since a larger S_w value [and therefore a smaller slope of Eq. (1)] is expected for the low field (large τ) range, where domain wall propagation dominates.

On the falling edge of the pulse, the different switching times measured for the two magnetic layers can be explained by Eq. (1). For the $Ni_{80}Fe_{20}$ layer, the effective reverse field ($H_{\text{eff}} = H_{\text{bias}} + H_{\text{dip}}$) is much larger than the static coercive field, leading to a fast reversal (less than 2 nsec). In the case of cobalt, H_{eff} is closer to the static coercivity leading to a slower dynamics.

Our next application of time-resolved XMCD deals with a series of $Co(5\text{ nm})/Cu/Ni_{80}Fe_{20}(5\text{ nm})$ spin valves grown by molecular beam epitaxy [18]. For 6 and 8 nm of Cu, the magnetic layers display parallel alignment by direct exchange, probably due to the presence of pinholes in the Cu layer. The quasistatic magnetization cycles, measured by classical magnetometry as well as by XMCD (Fig. 2), show that Co and $Ni_{80}Fe_{20}$ reverse simultaneously with coercive fields H_c of 4–5 mT. For 10 nm of Cu the magnetic coupling is weaker and two separate hysteresis

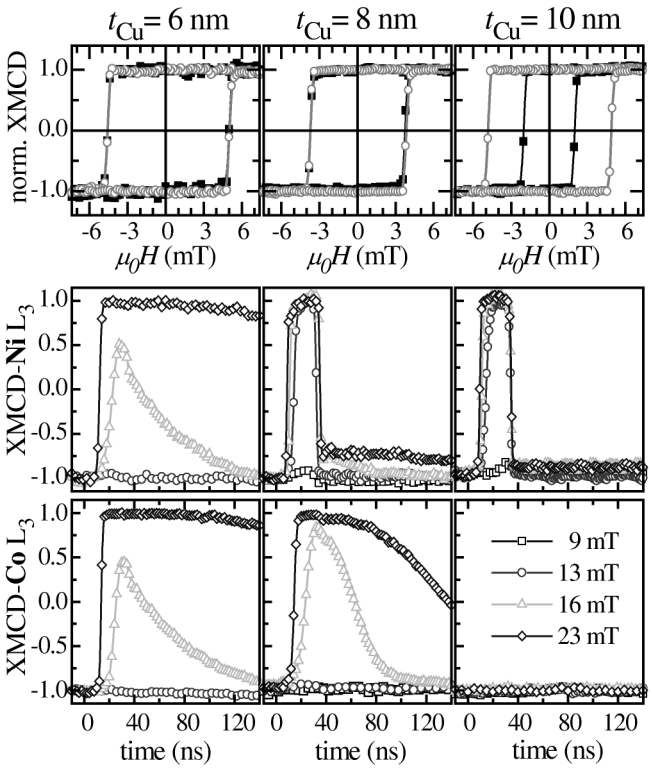

FIG. 2. Static and dynamic measurements in Co(5 nm/Cu/$Ni_{80}Fe_{20}$(5 nm) trilayers (t_{Cu} = 6, 8, and 10 nm). Top: site-selective hysteresis loops measured by XMCD for the Co (open dots) and $Ni_{80}Fe_{20}$ (squares) layers. Bottom: Dynamical response of the permalloy layer (top) and cobalt layer (bottom) to fields ($H_{pulse} + H_{bias}$) of amplitude 9 to 23 mT and width 30 ns ($H_{bias} = -5$ mT).

curves, with H_c of 3 and 5 mT, are measured for $Ni_{80}Fe_{20}$ and Co layers, respectively.

The results of the measurements obtained with 30-ns-long pulses are also shown in Fig. 2. The 10 nm Cu sample displays a behavior qualitatively similar to the tunnel junctions described above. The cobalt magnetization does not switch for pulses up to 23 mT. The $Ni_{80}Fe_{20}$ switches completely for fields around 10 mT, and its speed of reversal increases with the pulse amplitude. The two magnetic layers are clearly decoupled as expected from the quasistatic measurements.

For 6 nm of Cu, the Co and $Ni_{80}Fe_{20}$ layers switch in the same pulsed field and the dynamic responses of the two layers are exactly superposed. The permalloy layer magnetization relaxes with the same switching times as the Co layer, to which it is strongly coupled.

The 8 nm Cu sample displays the most interesting behavior. While in the quasistatic regime the two FM layers reverse simultaneously in a field of 5 mT, with 30-ns-long pulses the two metallic layers reverse in different fields. Similar to the case of the MTJ, on the rising edge of the pulse the two layers reverse with different speeds, the $Ni_{80}Fe_{20}$ magnetization reversing well before Co. On the falling edge, we retrieve for Co a slower magnetization decay. These results indicate that on this time scale the two layers are mostly uncoupled. The tail of the magnetization decay of $Ni_{80}Fe_{20}$ shows, however, that a fraction (about 15%) of its magnetization remains coupled to Co. These data show that whereas in the static regime the Co and $Ni_{80}Fe_{20}$ magnetizations are always parallel, for short pulses there is a field range where a nearly antiparallel configuration can be achieved.

This behavior may be explained if we suppose that the Co and permalloy layers consist of a weakly and a strongly coupled volume. The strongly coupled volume, where exchange interaction dominates, increases as the Cu spacer thickness decreases, probably through the formation of pinholes. When the exchange coupled volume dominates (6 nm Cu sample), the layers reverse together. In the intermediate case of 8 nm Cu layer, the strongly coupled volume is reduced. In the quasistatic regime, where domain wall propagation dominates, the domain walls are pinned by regions in the permalloy which are strongly coupled to the Co, and the coercivity is determined by these strongly coupled regions. The two layers switch simultaneously. For 30-ns-long pulses, nucleation of reversed domains is dominating, resulting in an easier switching of the whole weakly coupled region, giving rise to a permalloy coercivity smaller than the one of Co. In the absence of direct coupling (10 nm Cu sample), the two layers reverse independently both in the static regime and for short pulses.

As a last illustration of this technique we focus here on magnetic squares of side 1.3 μm patterned from the Co(15 nm)/Al_2O_3(2 nm)/$Ni_{80}Fe_{20}$(5 nm) MTJ studied above. The main interest of this kind of patterned structures is their possible application in nonvolatile MRAM. In contrast with the continuous film, the two FM layers display in zero field a strong antiparallel (AP) coupling, due to the strong dipolar field acting through the sides of the squares. This AP coupling is clearly shown in quasistatic hysteresis loops measured by XMCD for the two FM layers (inset of Fig. 3).

Time-resolved XMCD measurements were carried out for several values of the static bias field. Here we report on the results obtained for a bias of -8 mT after a negative saturation of the Co layer (Fig. 3). This field corresponds to the static coercive field of the $Ni_{80}Fe_{20}$ layer which is essentially defined by the dipolar field induced by Co.

The time-dependent data indicate that the switching process in the microstructured film is very different from the one observed for the continuous films (Fig. 1). The time-dependent magnetization obtained for the cobalt layer follows the time dependence of the pulsed field. For each field pulse, part of the magnetization reverses and, after a time of around 10 ns, "saturates" at a value which increases as the field amplitude increases. We attribute this behavior to a distribution of coercive fields among the magnetic dots. As the field amplitude increases more and more dots reverse. Since the switching time is shorter than the pulse duration, a plateau is found in the magnetic response.

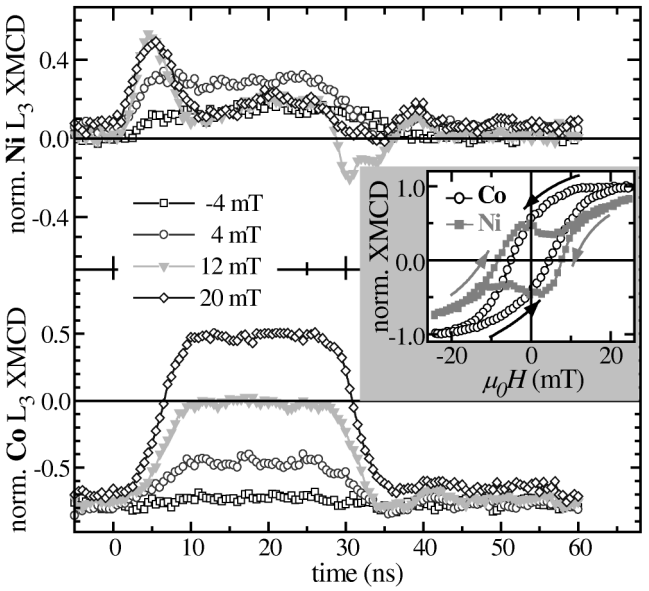

FIG. 3. Dynamical response of the permalloy and cobalt layers to pulsed fields of increasing amplitudes, in the presence of a bias field of -8 mT, for a series of 1.3 μm large square dots of $Co/Al_2O_3/Ni_{80}Fe_{20}$. The field amplitudes in the legends are $(H_{\text{pulse}} + H_{\text{bias}})$. Inset: hysteresis loops measured by XMCD for the Co and $Ni_{80}Fe_{20}$ layers. Note that for weak fields the two cycles are opposite due to the antiparallel alignment induced by the strong dipolar coupling.

When the pulse amplitude is not high enough to affect the cobalt, the switching behavior of $Ni_{80}Fe_{20}$ is similar to that just described for the Co layer. For an intermediate range of pulse amplitudes the $Ni_{80}Fe_{20}$ dynamics shows a complex behavior which is determined by the coupling with the Co layer. The $Ni_{80}Fe_{20}$ magnetization switches first, followed by the Co layer. The dipolar field from Co acting on $Ni_{80}Fe_{20}$ is now opposite to the pulsed field and part of the $Ni_{80}Fe_{20}$ magnetization is pulled back. A stable state is then maintained until the end of the pulse, where a symmetric situation is realized due to the faster response of $Ni_{80}Fe_{20}$ to the changing field. These results show that in such coupled magnetic structures, the dynamic reversal is a complex phenomenon and time-resolved XMCD appears as a unique probe to disentangle the magnetic response of each FM layer.

In conclusion, we have shown that time-resolved XMCD is an exceptional tool to study the dynamics of magnetization reversal with chemical selectivity. This probe cannot be competitive with other ultrafast techniques due to the limitation in time resolution ($\sim$100 ps). However, its strength has to be found in its unique capability to study independently the magnetization dynamics of each magnetic component of a complex heterostructure, as illustrated here for the coupled layers of spin-valve and tunnel junction systems. The difference in the coupling of two magnetic layers in static and dynamic regimes is illustrated here for the first time thanks to the chemical selectivity of time-resolved XMCD.

The technique is particularly suited for the study of complex systems in which the coercivities of the individual magnetic components may not be clearly separated with macroscopic techniques or when the magnetic coupling modifies the dynamics of each individual component. We have treated here the case of transition-metal based systems, but the technique could be applied to a large variety of samples. For example, in coupled RE/TM (rare-earth/transition metal) multilayers or alloys, the magnetization dynamics of the $4f$ (and the $5d$) component of the RE magnetization could be compared to that of the $3d$ magnetization of the TM [19].

One of the major developments which we envisage for this technique is its implementation on a photoemission electron microscope, to carry out time-resolved and chemical selective magnetic microscopy with subnanosecond and nanometer resolutions.

We thank A. Encinas, F. Nguyen Van Dau, and A. Vaurès for helpful discussions. J. C. acknowledges the support of the European Community for a Marie Curie Fellowship (Contract No. HPMF-CT-1999-00151). M. B. thanks the CAPES (Brasil) for financial support.

*Present address: INFM–Dipartimento di Fisica, Politecnico di Milano, p. Leonardo da Vinci 32, 20133 Milano, Italy.
†Corresponding author.

[1] For a review see W. D. Doyle, S. Stinnett, C. Dawson, and L. He, J. Magn. Soc. Jpn. **22**, 91 (1998).
[2] W. K. Hiebert, A. Stankiewicz, and M. R. Freeman, Phys. Rev. Lett. **79**, 1134 (1997).
[3] M. R. Freeman, A. Y. Elezzabi, and J. A. H. Stotz, J. Appl. Phys. **81**, 4516 (1997).
[4] N. D. Rizzo, T. J. Silva, and A. B. Kos, Phys. Rev. Lett. **83**, 4876 (1999).
[5] R. H. Koch *et al.,* Phys. Rev. Lett. **81**, 4512 (1998).
[6] R. H. Koch *et al.,* Phys. Rev. Lett. **84**, 5419 (2000).
[7] B. Dieny, J. Magn. Magn. Mater. **136**, 335 (1994).
[8] S. S. P. Parkin *et al.,* J. Appl. Phys. **85**, 5228 (1999).
[9] C. H. Tsang *et al.,* IBM J. Res. Dev. **42**, 103 (1998).
[10] J. Stöhr, J. Magn. Magn. Mater. **200**, 470 (1999), and references therein.
[11] M. Bonfim *et al.,* J. Appl. Phys. **87**, 5974 (2000).
[12] M. Bonfim *et al.,* J. Synchrotron Radiat. **5**, 750 (1998).
[13] F. Sirotti *et al.,* J. Appl. Phys. **83**, 1563 (1998).
[14] K. Mackay, M. Bonfim, D. Givord, and A. Fontaine, J. Appl. Phys. **87**, 1996 (2000).
[15] M. Sussiau *et al.,* J. Magn. Magn. Mater. **165**, 1 (1997).
[16] F. Montaigne *et al.,* Appl. Phys. Lett. **76**, 3286 (2000).
[17] E. M. Gyorgy, J. Appl. Phys. **28**, 1011 (1957); **29**, 1709 (1958); **315**, 110 (1960).
[18] A. Encinas *et al.,* Appl. Phys. Lett. **71**, 3299 (1997).
[19] M. Münzenberg *et al.,* J. Magn. Magn. Mater. **220**, 195 (2000).